Interpretation of maps of geopotential anomaly for the deep Pacific Ocean

by Joseph L. Reid[1] and Robert S. Arthur

ABSTRACT

Maps of the anomaly of the geopotential distance between various deep isobaric surfaces in the Pacific have been prepared and briefly compared with such information and concepts of the deeper circulation as are available. This comparison can yield, with no peculiar or extreme assumptions about the absolute flow at any level, a qualitative scheme of deeper circulation that is consistent with such few postulates and measurements as are at hand. According to this scheme, the pattern of circulation recognized at the sea surface (subtropical anticyclonic gyres and subarctic cyclonic gyres) would appear to extend downward, though in a weaker form, to depths as great as 3000 meters, below which only the two subarctic gyres and two western boundary currents in the South Pacific can be identified. Below the sea surface the subtropical anticyclonic gyres retreat poleward at greater depths and are confined by the Marianas and Tonga-Kermadec ridges to the central ocean, with separate anticyclonic gyres appearing west of the ridges. There is a broad eastward (relative to the deeper water) flow in lower latitudes, and poleward flow is seen along the eastern boundaries in middle and high latitudes.

A qualitative interpretation of the poleward shift of the subtropical anticyclonic gyres is made through application of simple dynamical and boundary constraints common to models of ocean circulation and thermocline structure. A zonal wind stress pattern resulting from westerlies and trades is used. Density in and near the mixed surface layer is assumed to increase from equator to pole while density at the bottom is taken to be virtually uniform. The observed shift of anticyclones with depth is consistent with the interaction of a Sverdrup transport produced by the wind and the assumed boundary conditions on the density.

On the relative geostrophic flow

1. Introduction

The purpose of this study is to present maps of the anomaly of the geopotential distance between various deep isobaric surfaces in the Pacific Ocean, to consider them in terms of geostrophic shear, to compare them with the circulation recognized in the upper layer, and to discuss them briefly in terms of deep circulation.

A map of this quantity at the sea surface relative to the 1000-decibar surface was prepared by Reid (1961) for the Pacific Ocean, and a new one is presented here (Fig. 1) to accompany the deeper fields. Such maps for various areas of the South

1. Scripps Institution of Oceanography, La Jolla, California, 92037, U.S.A.

Pacific have also been prepared and discussed in more detail by Deacon (1937a), U.S. Navy Hydrographic Office (1957), Wyrtki (1962), Gordon (1967), Garner (1969), and Reid and Mantyla (1971).

These maps indicate geostrophic surface flows similar to the currents derived from direct calculations of the set and drift of vessels (U.S. Navy Hydrographic Office, 1944, 1947, 1950a, 1950b; Meteorological Office, 1967). Such currents have generally been accepted as being directly driven by the major wind systems (Munk, 1950; Welander, 1959), but thermohaline and topographical driving may also contribute (Holland, 1973).

2. The data

In the preparation of these maps about 7200 hydrographic stations have been considered, resulting from the work of more than 200 expeditions. Most of the observations were made by the vessels of 11 countries (Australia, Canada, Chile, Denmark, France, Germany, Japan, New Zealand, United Kingdom, U.S.A., and U.S.S.R.).

Most of the data were obtained through the U.S. National Oceanographic Data Center. The stations used are too numerous to list in detail.

Substantial improvements in the measurement of salinity and temperature have been made within the last 15 years, and wherever possible we have used the more recent data in the preparation of these maps. A great quantity of material has become available from various national and international cooperative programs such as the Cooperative Study of the Kuroshio, the U.S. Antarctic Research Program aboard the *Eltanin*, and the GEOSECS expedition. Major expeditions such as Scorpio, Southern Cross, Phoenix, the *Hudson* 70, and the *Gascoyne* 3/61 have supplied substantial quantities of material, as have many smaller-scale expeditions in various areas.

However, there are not enough modern data to prepare such maps, and it has been necessary to use data from as far back as the *Carnegie* and *Dana* work (in the 1920's) in some areas, and a substantial amount of Japanese work in the 1930's in others, as well as some of the earlier *Discovery* work in the Antarctic Ocean.

3. Limitations

The maps of the deeper fields presented here will be seen to be quite well defined by the available data in some areas and marginally defined, or not defined at all, in other areas. The gradients are strongest and the patterns best defined in higher latitudes, as might be expected, and weakest and the field least clear in the intertropical zone. The contour values chosen are not at regular intervals or at systematically varying intervals, as the gradients are highly variable; they have been chosen to illustrate the major features of the field in the simplest way.

Reed (1970), in his examination of the deep geopotential topography, gave error estimates (two standard deviations) of about 0.5 dynamic cm/1000 decibars for

random errors of ± 0.02°C in temperature and ± 0.01‰ in salinity. He notes that this does not take into account any systematic errors that may result from calibration and standardization problems. Such systematic errors can sometimes be identified (as when a long line of stations taken by one expedition is consistently different from several crossings by other vessels) and some elimination has been done on this basis. Of course, it has not been possible to identify and eliminate all erroneous data, and some of the choices made have perhaps been arbitrary. These choices, and the contouring over much of the area, must be considered subjective. It is noteworthy, however, that the maps presented here, which include considerable amounts of data made available since Reed's (1970) work, and which have been contoured independently of his, tend in general to extend and amplify his interpretations rather than to contradict them.

These maps are made from the best data available, and the coverage is quite good in some areas. As the figures will illustrate, the data define a strong and clear field south of about 20°S latitude. Later data and other interpretations are not likely to make major changes in that area.

At lower latitudes the field is, of course, much weaker, and the array of data there and in the Philippine Sea defines the field only marginally at best. Later data, or even another interpretation of the present data, might yield substantially different patterns in the huge area between about 50°N and 20°S. For this reason this paper will deal mostly with the South Pacific. The North Pacific is included here to illustrate what data are available and their general values in the area, and to permit a comparison of the patterns, even if marginally defined, with those in the South Pacific.

4. The maps

Instead of reproducing the earlier map of the anomaly of geopotential distance between the sea surface and the 1000-decibar surface (Reid, 1961), a new map, using data from the northern winter season only, has been prepared (Fig. 1). On both maps the major features of both the North Pacific and the South Pacific Ocean are (in each) a subarctic low (geopotential) cell (the southern low cell surrounding Antarctica), a subtropical high cell, and, extending zonally near the equator, a long narrow (and weaker) subequatorial high cell. These various cells are fairly consonant with the generally accepted concepts of West-Wind Drift in high latitudes, Trade-Wind Drift in low latitudes, with meridional flow along the eastern and western boundaries and some counter-flow in the intertropical zone.

The newer map differs from the earlier one in several ways, but only those new features that may be related to the deeper fields will be mentioned here.

One difference is the existence of a westward flow south of the Antarctic Circumpolar Current between about 140°W and 160°E (Reid and Mantyla, 1971). We take this new feature to be the result of simply having more data, not evidence of some seasonal change.

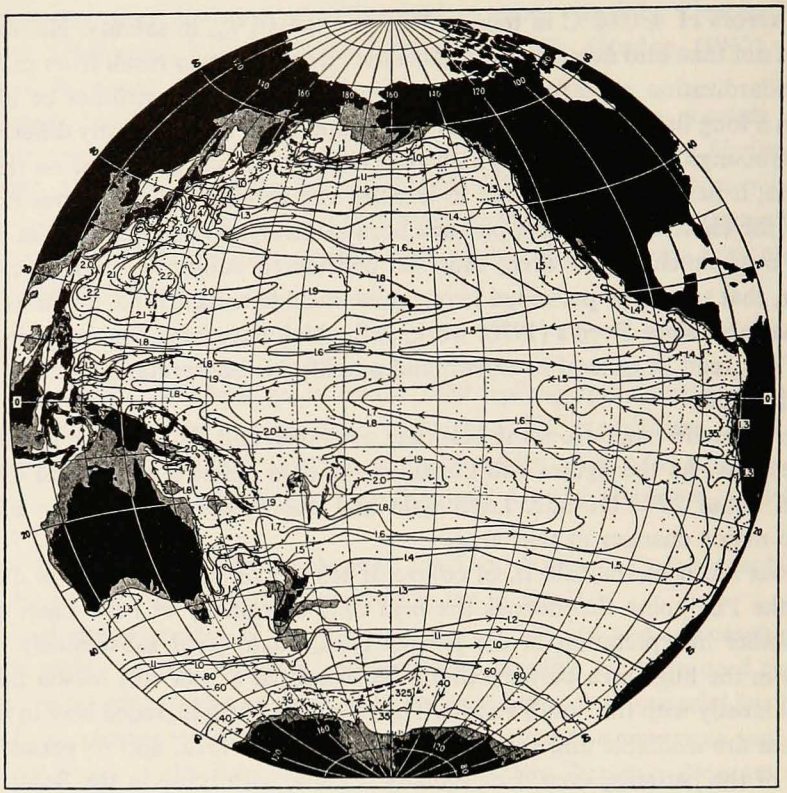

Figure 1. The geopotential anomaly at the sea-surface relative to the 1000-decibar surface, in dynamic meters (10 m^2/sec^2 or 10 J/kg). In the shaded areas the ocean depth is less than 1000 m.

Another difference is the added detail within the Philippine Sea. In Figure 1 most of the data in the area west of 155°E and north of 10°N are from the Cooperative Study of the Kuroshio expeditions carried out in the winter of 1965–1966 and have been illustrated in an atlas (Maritime Safety Agency, 1968). The observations were spaced more closely than those used earlier and present much more detail. In particular, the return (southwestward) flow offshore from the Kuroshio Current is much more complex, and a separate high cell is found near 22°N 145°E, overlying the South Honshu and Marianas ridges. Some part of this detail may be related to a subtropical countercurrent (Yoshida and Kidokoro, 1967), but there may also be a relation to the underlying north-south ridges seen on the following figures.

The maps presented here for the deeper isobars (Figs. 2–5) show fields that are progressively weaker at greater depths but still preserve the subarctic low cells even on the 3000/4000-decibar surface. The subtropical high cells are seen also down to the 2500/3500-decibar surface, but they are found progressively farther poleward at greater depths.

Where the narrow subequatorial high cells are seen just north and south of the

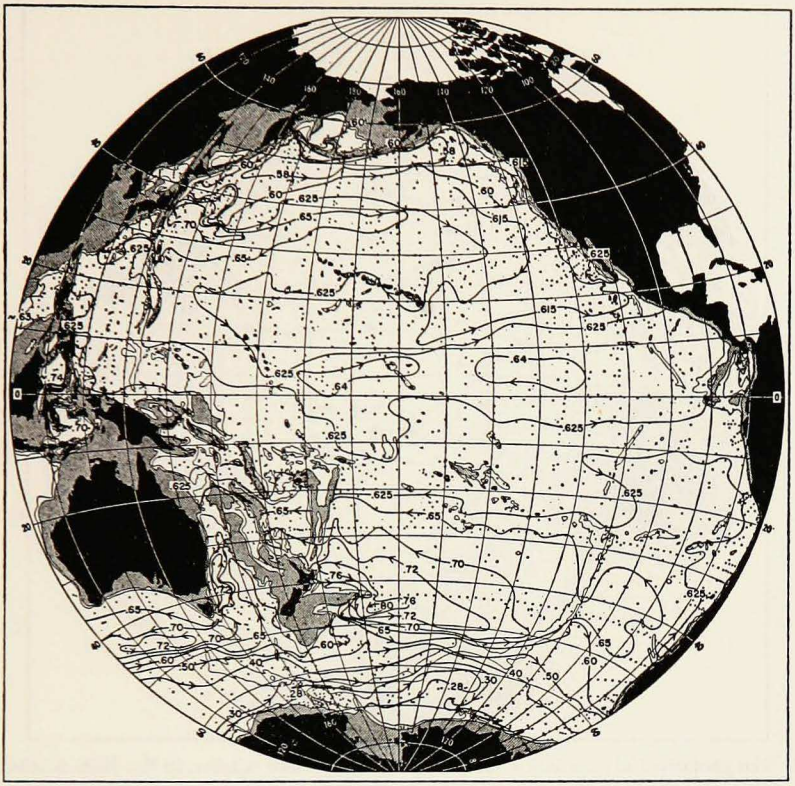

Figure 2. The geopotential anomaly at the 1000-decibar surface relative to the 2000-decibar surface, in dynamic meters (10 m^2/sec^2 or 10 J/kg). In the shaded areas the ocean depth is less than 2000 m, and the light line is the 3000-m depth contour.

equator on the 0/1000-decibar map (Fig. 1), there is only one such cell on the 1000/2000-decibar map (Fig. 2), but it is wider there; on the 2000/3000-decibar map (Fig. 3) it is wider still, broadening as the two subtropical highs retreat poleward. It cannot be detected on the deepest map (Fig. 5).

At greater depth the various cells show some effects from the bottom topography. On the 1000/2000-decibar surface the Tonga-Kermadec Ridge extending northward from New Zealand separates the southern subtropical anticyclonic gyre into two parts, the principal part in the central South Pacific Ocean and a separate smaller part in the Tasman Sea, and the East Pacific Rise may also separate a cell in the eastern area. The Marianas Ridge, extending southward from Japan, separates the northern subtropical gyre on the 2000/3000-decibar surface. On the deeper maps both the central anticyclonic gyres are completely separated by these ridges from separate gyres within the Philippine Sea and Tasman Sea.

Figure 3. The geopotential anomaly at the 2000-decibar surface relative to the 3000-decibar surface, in dynamic meters (10 m^2/sec^2 or 10 J/kg). In the shaded areas the ocean depth is less than 3000 m.

5. Interpretation in terms of relative geostrophic flow

Within the limitations of the data and the geostrophic approximation, each of these maps may be assumed to represent the geostrophic shear between two pressure surfaces, or the flow along one relative to the other. On each of the maps the arrows indicate the sense of flow at the upper surface relative to the deeper surface.

In the earlier paper discussing the geostrophic flow at the sea surface relative to the 1000-decibar surface (Reid, 1961), it was possible to compare the field with the available direct measurements of surface flow. Using this field under the assumption that the flow at the 1000-decibar surface is weaker than at the sea surface gives the correct sense of surface flow nearly everywhere, and identifies the major gyres and the areas of high and low velocity.

It does not follow that for each of the maps presented here the flow is always weaker at the greater pressure. And there is no large fund of current measurements below the surface that can be used to evaluate the maps in terms of flow. The only information available for testing there comes from the distributions of various characteristics (cold abyssal water coming north from the Antarctic, saline and oxygen-poor water moving poleward beneath the surface along parts of the eastern

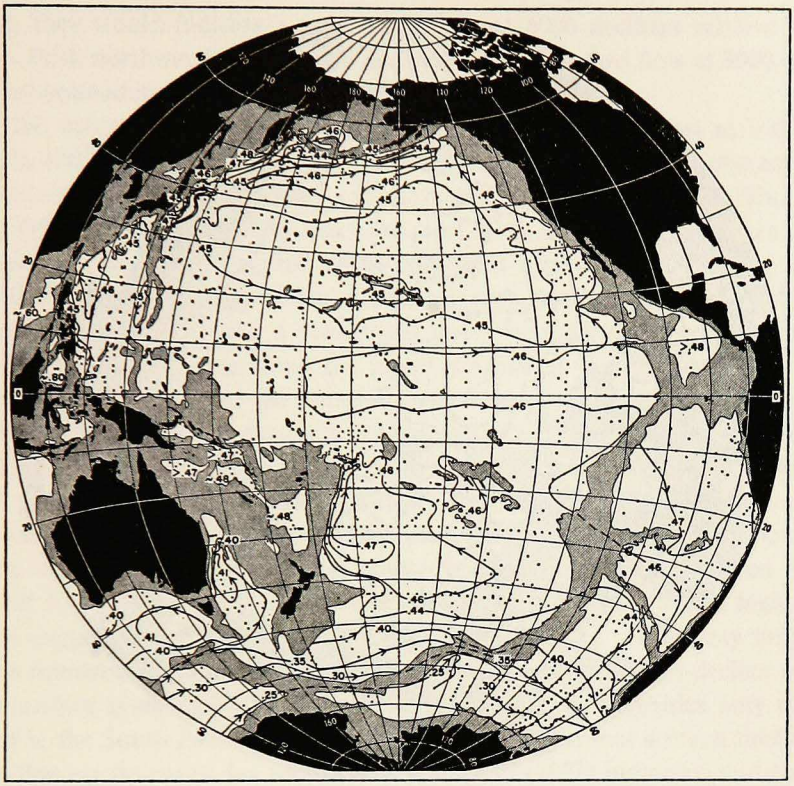

Figure 4. The geopotential anomaly at the 2500-decibar surface relative to the 3500-decibar surface, in dynamic meters (10 m^2/sec^2 or 10 J/kg). In the shaded areas the ocean is less than 3500 m.

boundary, and tonguelike features at intermediate depths extending around the principal anticyclonic gyres).

That the Antarctic Circumpolar Current extend all the way to the bottom has been generally accepted on the basis of the measured water characteristics. In this high-latitude domain the meridional gradients are strong, and the maps will provide a correct sense of flow if the eastward speed is assumed to decrease toward the bottom. Likewise, a strong northward abyssal flow has been postulated along the eastern side of the Tonga-Kermadec Ridge, both from the distribution of characteristics (Wüst, 1929; Wooster and Volkmann, 1960; Reid *et al.*, 1968; Reid and Lynn, 1971; Warren, 1973; Mantyla, in press) and from direct measurements (Reid, 1969; Warren and Voorhis, 1970; Reid and Lonsdale, 1974). In addition, an immediately overlying southward flow, returning the bottom waters that have entered the North Pacific from the south and been made nutrient-rich and oxygen-poor, has been proposed.

The possibility of a southward flow of water out of the South Pacific immediately above the incoming deep and bottom water was proposed by Wüst (1929) on the

Figure 5. The geopotential anomaly at the 3000-decibar surface relative to the 4000-decibar surface, in dynamic meters (10 m^2/sec^2 or 10 J/kg). In the shaded areas the ocean depth is less than 4000 m.

basis of salinity distribution and by Deacon (1937b) on the basis of the oxygen distribution. More recently, Craig *et al.* (1972), Gordon (in press), and Reid (1973a) have discussed the possibility of a southward flow east of the Kermadec Ridge above the incoming abyssal flow. The Scorpio plates (Stommel *et al.*, 1973) illustrate both the basic oxygen and salinity characteristics that first suggested a return flow at this level and the greater detail that has suggested this is a flow along the western boundary. Reid and Lonsdale (1974) report direct measurements of the abyssal northward flow near 10°S (the Samoan Passage) and have shown that both these measurements and the associated water characteristics are consonant with a return flow of water southward along the Tonga Ridge at depths near 3000 m. Farther south the southward flow appears to take place at shallower depths; along the Tonga-Kermadec Ridge the oxygen concentrations suggest a southward flow above about 3000 m depth near 28°S and above about 2500 m depth near 43°S (Scorpio sections; Stommel *et al.*, 1973), with northward flow beneath. These two flows are consonant with the the shear in that area on the 3000/4000-decibar map (Fig. 5). As drawn, the arrows indicate a southward flow at 3000 decibars relative to 4000 decibars;

reversed, they would indicate a northward flow at 4000 decibars relative to 3000 decibars. Both northward flow at 4000 decibars and southward flow at 3000 decibars can be accommodated within the field observed.

That the subtropical high cells correspond to anticyclonic gyres at least down to 1000 to 1500 m seems fairly clear from the comparisons with water characteristics. This domain has been illustrated and discussed by Reid (1965; 1973b; 1973c), Barkley (1968), Tsuchiya (1968), and Johnson (1973), and the distributions of heat, salt, oxygen, and nutrients appear to be consistent with such anticyclonic flow.

In Callahan's (1972) study of the salt and oxygen distributions on two deep isopycnal surfaces, he proposed a substantial southward flow of oxygen-poor water from the intertropical zone along the coast of Chile as one of the sources of the low oxygen values found in the upper layers of the Circumpolar Current. His two isopycnals lay near 1600 meters and 3500 meters depth in the area near the coast of Chile. The shear on the 2000/3000-decibar map and the 2500/3500-decibar map (Figs. 3 and 4) is consistent with such flow, with the speed decreasing downward.

Poleward subsurface flows have been postulated along the eastern boundaries since the work of Gunther (1936) off South America and of Sverdrup and Fleming (1941) off North America. In both cases the evidence offered was the high salinity and low oxygen values found in the middle latitudes, and presumably originating from the intertropical zone. Referring the overlying flow to the 500-decibar or 1000-decibar surface gives such a flow in the North Pacific but provides only marginal evidence in the South Pacific. From these maps it appears that a much thicker layer may be flowing poleward [as the work of Callahan (1972) indicates] and the shear may be too weak for such shallower references to be useful.

6. The general circulation

If the maps presented here are assumed to represent the field of geopotential fairly well, then no peculiar or extreme assumptions need be made about the absolute flow at any level in order for these maps to provide a qualitative scheme of deeper circulation that is consistent with such few measurements and postulates as are at hand.

According to this scheme, the pattern of circulation recognized at the sea surface would appear to extend downward in a weakened but otherwise only moderately modified form to depths as great as 3000 m, below which only the subarctic gyres and two western boundary currents in the South Pacific can be identified.

At increasing depths the subtropical anticyclonic gyres retreat poleward, and a broad eastward (relative to deeper isobars) flow obtains in the lower latitudes.

Some fairly clear evidence for poleward flow along the eastern boundary in middle and high latitudes is seen, though on the deepest map (Fig. 5) the pattern is not defined within the Chile Basin.

At the greater depths, the Marianas and Tonga-Kermadec ridges cut off the

subtropical anticyclonic gyres from the western Pacific, but separate anticyclonic features are found in the Tasman Sea and in the Philippine Sea: there is some suggestion of such a feature east of the East Pacific Rise on the 2000/3000-decibar map.

In the Philippine Sea the 1000/2000-decibar field (Fig. 2) appears to be quite different from the 2000/3000-decibar field (Fig. 3). On the deeper field there is a fairly continuous northward flow along the western boundary and a southward flow just west of the Marianas Ridge. On the shallower surface (Fig. 2) the Kuroshio is evident only as part of a small gyre just south of Japan. This difference may be only a consequence of inadequacies of the available data or it may be a real feature, indicating a very weak shear at 1000 decibars relative to 2000 decibars.

The deeper fields (Figs. 2–5) all show a substantial effect of the ridges extending southward from Japan (between 140°E and 150°E). Perhaps some of the complexity seen on the surface map (Fig. 1) in that area is also an effect of these ridges, as well as of the wind field discussed by Yoshida and Kidokoro (1967). The available array of data cannot define a meridional flow on either side of the ridges; it does not preclude such a flow.

7. The subtropical high cells in other oceans

The poleward shift of the subtropical high cells that is a prominent feature of these maps is also apparent in the South Atlantic in the maps of σ_t (Wüst and Defant, 1936) and in Defant's (1941) relative topography of the Atlantic; it is detected most easily in the maps of the depths of σ_t surfaces prepared by Montgomery and Pollak (1942), and is also apparent in the maps of surfaces of constant potential density prepared by Buscaglia (1971). There is also some suggestion of a separation of the South Atlantic high cell by the Mid-Atlantic Ridge.

Wyrtki's (1971) maps of geopotential anomaly in the Indian Ocean show the same poleward shift; there is also the possibility that the distortions of the subtropical anticyclone observed at greater depths in the South Indian Ocean are a consequence of the topography there. (The topography of the Indian Ocean is more complicated; that is, the sill depths are shallower and the basins are more numerous and smaller than in the South Pacific, and thus the relation of topography to geopotential anomaly is more difficult to determine.)

Comments on the poleward shift of the subtropical anticyclonic gyres

The subtropical anticyclonic patterns of pressure represented in the maps of geopotential anomaly are, of course, determined by the distribution of observed density from which the maps were calculated. Isolines of density at intermediate depths in a meridional section through such anticyclones tend to show a rise toward the poles and the equator with maximum depth in the subtropics, and the points of maximum depth shift poleward as we progress to deeper isopycnals.

We consider some dynamics that may be operative in the observed vertical structure

of the density field and the anticyclones. The structure is reproduced in certain three-dimensional (3-D) numerical models of ocean circulation, e.g., in the models of Bryan and Cox (1968a: Figs. 11, 12, 14) and Gill and Bryan (1971: Figs. 8, 13), and an explanation could be sought from the framework of the models. Various thermocline models, e.g. the one used by Welander (1971), exhibit features of the structure, but these models do not satisfy complete boundary conditions as has been pointed out (Veronis, 1973). Nevertheless, they, like the 3-D numerical models, provide clues about the basis for the observed structure.

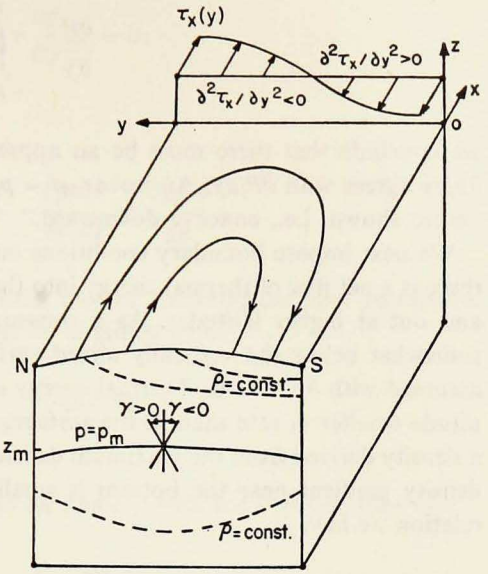

Figure 6. Schematic block diagram showing zonal wind stress, $\tau_x(y)$, and corresponding Sverdrup transport streamlines (isolines with arrows at sea surface). Meridional section shows isobar ($p = p_m$) at mean depth z_m and isopycnals (ϱ = const.). Tilt lines for equatorward ($\gamma < 0$) or poleward ($\gamma > 0$) shift of centers of anticyclones with depth are indicated.

The appearance of the structure in various models and in the ocean suggests the possibility of a direct qualitative interpretation through application of simple dynamical and boundary constraints. Wind-driving will be combined with thermohaline considerations. Let the wind be zonal with westerlies in the higher latitudes and easterlies in the lower latitudes of a subtropical β-plane ocean (Fig. 6). We assume a northern hemisphere meridional boundary across which there is zero integrated mass transport and invoke the Sverdrup (1947) transport relations to the west of the boundary (note that $x < 0$),

$$M_x = \frac{x}{\beta}\frac{\partial^2\tau_x}{\partial y^2}, \quad M_y = -\frac{1}{\beta}\frac{\partial\tau_x}{\partial y},$$

$$\frac{\partial P}{\partial y} = -\frac{fx}{\beta}\frac{\partial^2\tau_x}{\partial y^2},$$

where M_x and M_y are the eastward and northward transports, respectively; P is the integral of the pressure, p, from great depth ($z = -H$) to the surface ($z = \eta$); f is the Coriolis parameter; and $\beta = df/dy$ is taken as constant. If the wind stress $\tau_x(y)$ has derivatives that change sign as indicated in Fig. 6, then the streamlines of mass transport show anticyclonic curvature and $\partial P/\partial y$ changes from positive values in the southern part of the ocean to negative in the northern part. Since

$$\frac{\partial P}{\partial y} = \int_{-H}^{\eta} \frac{\partial p}{\partial y} dz,$$

we conclude that there must be an appreciable range of depth where the sign of $\partial p/\partial y$ agrees with $\partial P/dy$. An isobar, $p = p_m$, in this depth range must have the curvature shown, i.e., concave downward.

We next impose boundary conditions on the density distribution. On the average there is a net flux of thermal energy into the ocean across the surface in low latitudes and out at higher latitudes. As a consequence, we assume that $\partial \varrho/\partial y > 0$ in and somewhat below the vertically mixed surface layer. Furthermore, a stable state is assumed with $\partial \varrho/\partial z < 0$. Thermal energy exchange at the bottom is orders of magnitude smaller in rate than at the surface, and we expect the bottom water to have a density derived from the maximum density at the surface. Therefore, the horizontal density gradient near the bottom is small, i.e., $\partial \varrho/\partial y \doteq 0$. From the hydrostatic relation we have

$$\frac{\partial p}{\partial y} = -g \int_{-H}^{z_m} \frac{\partial \varrho}{\partial y} dz$$

for the y-component of pressure gradient at the mean level z_m of isobar p_m, if the gradient at $z = -H$ is negligible. Considering the curvature of p_m and the small gradient $\partial \varrho/\partial y$ near $z = -H$, we conclude that for an appreciable range of depth below z_m the isopycnals must have a reverse curvature to p_m, i.e., concave upward.

In this regard it is useful to consider the vertical structure of the Sverdrup transport as interpreted by Stommel (1957). The wind stress in our example produces an Ekman transport in the surface waters that is generally convergent. The convergence causes a rise of the free surface from the northern and southern boundaries to the center of the gyre and a slow downward movement of water from surface to subsurface depths. The water below the Ekman layer moves geostrophically and with an equatorward component in order that the geostrophic divergence may gradually reduce the vertical movement to zero at great depth. With the stress distribution in the example, the convergence and downward motion is larger at midlatitudes of the transport gyre. The concave shape of the isopycnals at depth is consistent with the downward motion of this less dense water and with the production of zero pressure gradient at $z = -H$ through density compensation.

Near the surface, the maximum depth of isopycnals must shift to the southern end of the section in conformity with the boundary condition $\partial \varrho/\partial y > 0$. This shift causes a reduction in the slope of the southern portion of upper isobars, i.e., a shift toward the equator in the crests of successive isobars. A quantitative relation may be obtained for the tilt of a line drawn through successive crests. In the vertical section, for zero pressure change, we have

$$dp = \frac{\partial p}{\partial y} dy + \frac{\partial p}{\partial z} dz = 0.$$

The slope of an isobar is given by

$$i_p = \left(\frac{dz}{dy}\right)_{p = \text{const.}} = -\frac{\partial p/\partial y}{\partial p/\partial z} = \frac{\partial p/\partial y}{\varrho g},$$

where the hydrostatic approximation has been used in obtaining the final expression. The tilt of the line along which $i_p = 0$ may be obtained from

$$0 = \frac{\partial^2 p/\partial y^2}{\varrho g} dy + \frac{\partial^2 p/\partial z \partial y}{\varrho g} dz.$$

If the line through successive crests makes an angle γ with the vertical, then

$$\tan\gamma = \left(\frac{dy}{dz}\right)_{i_p = 0} = -\frac{\dfrac{\partial}{\partial y}(\partial p/\partial z)}{\partial^2 p/\partial y^2} = \frac{g\,\partial\varrho/\partial y}{\partial^2 p/\partial y^2},$$

where the hydrostatic approximation has again been used. Since $\partial^2 p/\partial y^2 < 0$ and $\partial\varrho/\partial y > 0$ near the surface layer, we have $\gamma < 0$ and we verify that anticyclones and high pressure ridges shift equatorward (toward lower density) as we approach the surface. A comparable relation has long been applied in the atmosphere (Haltiner and Martin, 1957).

We conclude that the observed shift of anticyclones with depth is consistent with the interaction of a Sverdrup transport produced by the wind and a density distribution satisfying the assumed boundary conditions and the constraints of the transport. The adequacy of the simplified dynamics of the Sverdrup approximation may, of course, be questioned. It is reassuring to note that the Sverdrup balance dominates over a considerable portion of the subtropical anticyclones in some full 3-D models (Bryan and Cox, 1968b: Fig. 1; Gill, 1971: Fig. 13). Therefore, our qualitative discussions may have properly selected the operative dynamical and boundary constraints. However, we must keep in mind that major gyres may result from a combination of thermohaline-driving and topographic features (Holland, 1973).

The models are capable of giving a variety of information about the structure (Gill, 1971). For example, the motion across isopycnals could be determined. Results are likely to depend critically on the values of scaling parameters in the models and there are computational problems that limit the freedom to choose the most appropriate values of parameters for modeling the real ocean. Qualitative conclusions may be more secure than detailed quantitative results.

Acknowledgements. The authors wish to express their appreciation to Professor Montgomery for fruitful and pleasant discussions on many oceanographic topics over the years, and to acknowledge the encouragement and guidance he has given. The work reported here was supported by the National Science Foundation, the Office of Naval Research, and by the Marine Life Research Program, the Scripps Institution's component of the California Cooperative Fisheries Investigations, a project sponsored by the Marine Research Committee of the State of California. The authors are grateful for comments from George Veronis and referees.

REFERENCES

Barkley, R. A. 1968. Oceanographic atlas of the Pacific Ocean. Univ. Hawaii Press, Honolulu, 20 pp., 156 figs.

Bryan, K. and M. D. Cox. 1968a. A nonlinear model of an ocean driven by wind and differential heating: Part I. Description of the three-dimensional velocity and density fields. J. Atmos. Sci., *25*(6): 945–967.

Bryan, K. and M. D. Cox. 1968b. A nonlinear model of an ocean driven by wind and differential heating: Part II. An analysis of the heat, vorticity and energy balance. J. Atmos. Sci., *25*(6): 968–978.

Buscaglia, J. L. 1971. On the circulation of the Intermediate Water in the southwestern Atlantic Ocean. J. Mar. Res., *29*(3): 245–255.

Callahan, J. E. 1972. The structure and circulation of Deep Water in the Antarctic. Deep-Sea Res., *19*(3): 563–575.

Craig, H., Y. Chung and M. Fiadeiro. 1972. A benthic front in the South Pacific. Earth & Planet. Sci. Lett., *16*: 50–65.

Deacon, G. E. R. 1937a. Note on the dynamics of the Southern Ocean. Discovery Rep., *15*: 125–152.

Deacon, G. E. R. 1937b. The hydrology of the Southern Ocean. Discovery Rep., *15*: 1–124.

Defant, A. 1941. Die relative Topographie einzelner Druckflachen in Atlantischen Ozean. Wiss. Ergebn. dtsch. atlant. Exped. "Meteor", *6*(2)(4): 183–190.

Garner, D. M. 1969. The geopotential topography of the ocean surface around New Zealand. N.Z. J. Mar. Freshwat. Res., *3*(2): 209–219.

Gill, A. E. 1971. Ocean models. Phil. Trans. R. Soc. Lond. A, *270*: 391–413.

Gill, A. E. and K. Bryan. 1971. Effects of geometry on the circulation of a three-dimensional southern-hemisphere ocean model. Deep-Sea Res., *18*(7): 685–722.

Gordon, A. L. 1967. Structure of Antarctic waters between 20°W and 170°W. Antarctic Map Folio Series, Folio 6, edited by V. C. Bushnell. Amer. Geogr. Soc., New York, 10 pp., 14 plates.

Gordon, A. L. In press. General ocean circulation. Proc. Symp. Numerical Models of Ocean Circulation, Nat. Acad. Sci., Durham, N. H., October 1972. Nat. Acad. Sci., Washington, D.C.

Gunther, E. R. 1936. A report on the oceanographical investigations in the Peru coastal current. Discovery Rep., *13*: 107–276.

Haltiner, G. J. and F. L. Martin. 1957. Dynamical and physical meteorology. McGraw-Hill, New York, 470 pp.

Holland, W. R. 1973. Baroclinic and topographic influences on the transport in western boundary currents. Geophys. Fluid Dyn., *4*: 187–210.

Maritime Safety Agency, Hydrogr. Div., Japanese Oceanographic Data Center. 1968. Provisional CSK Atlas, Vol. 2 – Winter 1965–66, 44 pp.

Johnson, R. E. 1973. Antarctic Intermediate Water in the South Pacific Ocean. In *Oceanography of the South Pacific 1972*. Compiler, R. Fraser. New Zealand National Commission for UNESCO, Wellington, 524 pp.

Mantyla, A. W. In press. Abyssal Pacific circulation inferred from bottom potential temperature distribution.

Meteorological Office. 1967. Quarterly surface current charts of the South Pacific Ocean. Met. O. 435 (2nd edition), 25 pp.

Montgomery, R. B. and M. J. Pollak. 1942. Sigma-T surfaces in the Atlantic Ocean. J. Mar. Res., *5*(1): 20–27.

Munk, W. H. 1950. On the wind-driven ocean circulation. J. Met., *7*(2): 79–93.

Reed, R. K. 1970. Geopotential topography of deep levels in the Pacific Ocean. J. Oceanogr. Soc. Japan, *26*(6): 331–339.

Reid, J. L., Jr. 1961. On the geostrophic flow at the surface of the Pacific Ocean with respect to the 1000-decibar surface. Tellus, *13*(4): 489–502.

Reid, J. L., Jr. 1965. Intermediate waters of the Pacific Ocean. Johns Hopk. Oceanogr. Stud., *2*: 85 pp.

Reid, J. L. 1969. Preliminary results of measurements of deep currents in the Pacific Ocean. Nature, *221*(5183): 848.

Reid, J. L. 1973a. Transpacific hydrographic sections at Lats. 43°S and 28°S: the SCORPIO Expedition–III. Upper water and a note on southward flow at mid-depth. Deep-Sea Res., *20*(1): 39–49.

Reid, J. L. 1973b. The shallow salinity minima of the Pacific Ocean. Deep-Sea Res., *20*(1): 51–68.

Reid, J. L. 1973c. Northwest Pacific Ocean waters in winter. Johns Hopk. Oceanogr. Stud., *5*: 96 pp.

Reid, J., Jun., H. Stommel, E. D. Stroup, B. A. Warren. 1968. Detection of a deep boundary current in the western South Pacific. Nature, *217*: 937.

Reid, J. L. and R. J. Lynn. 1971. On the influence of the Norwegian-Greenland and Weddell seas upon the bottom waters of the Indian and Pacific oceans. Deep-Sea Res., *18*(11): 1063–1088.

Reid, J. L. and A. W. Mantyla. 1971. Antarctic work of the Aries expedition. Antarctic J., U.S., *6*(4): 111–113.

Reid, J. L. and P. F. Lonsdale. 1974. On the flow of water through the Samoan Passage. J. Phys. Oceanogr., *4*(1): 58–73.

Stommel, H. 1957. A survey of ocean current theory. Deep-Sea Res., *4*(3): 149–184.

Stommel, H., E. D. Stroup, J. L. Reid and B. A. Warren. 1973. Transpacific hydrographic sections at Lats. 43°S and 28°S: the SCORPIO Expedition–I. Preface. Deep-Sea Res., *20*(1): 1–7.

Sverdrup, H. U. 1947. Wind-driven currents in a baroclinic ocean: with application to the Equatorial Currents of the Eastern Pacific. Proc. Nat. Acad. Sci., Wash., *33*(11): 318–326.

Sverdrup, H. U. and R. H. Fleming. 1941. The waters off the coast of Southern California, March to July, 1937. Bull. Scripps Instn. Oceanogr., *4*(10): 261–378.

Tsuchiya, M. 1968. Upper waters of the intertropical Pacific Ocean. Johns Hopk. Oceanogr. Stud., *4*: 50 pp.

U.S. Navy Hydrographic Office. 1944. Atlas of current charts, southwestern Pacific Ocean. H.O. Pub. 568, 11 plates.

U.S. Navy Hydrographic Office. 1947. Atlas of surface currents, northeastern Pacific Ocean. H.O. Pub. 570, 12 plates.

U.S. Navy Hydrographic Office. 1950a. Atlas of surface currents, northwestern Pacific Ocean. H.O. Pub. 569, 12 plates.

U.S. Navy Hydrographic Office. 1950b. Atlas of pilot charts, Pacific and Indian oceans. H.O. Pub. 577, 16 plates.

U.S. Navy Hydrographic Office. 1957. Oceanographic atlas of the polar seas. Part 1: Antarctic. H.O. Pub. 705, Pt. 1, 70 pp.

Veronis, G. 1973. Large scale ocean circulation. *In* Advances in Applied Mechanics, Vol. 13, edited by C.-S. Yih. Academic Press, New York, 342 pp.

Warren, B. A. 1973. Transpacific hydrographic sections at Lats. 43°S and 28°S: the SCORPIO Expedition–II. Deep water. Deep-Sea Res., *20*(1): 9–38.

Warren, B. A. and A. D. Voorhis. 1970. Velocity measurements in the deep western boundary current of the South Pacific. Nature, *228*(5274): 849–850.

Welander, P. 1959. On the vertically integrated mass transport in the oceans. *In* The Atmosphere and the Sea in Motion, Scientific Contributions to the Rossby Memorial Volume, edited by B. Bolin. Rockefeller Inst. Press, New York, 509 pp.

Welander, P. 1971. Some exact solutions to the equations describing an ideal-fluid thermocline. J. Mar. Res., *29*(2): 60–68.

Wooster, W. S. and G. H. Volkmann. 1960. Indications of deep Pacific circulation from the distribution of properties at five kilometers. J. Geophys. Res., *65*(4): 1239–1249.

Wüst, G. 1929. Schichtung und Tiefenzirkulation des Pazifischen Ozeans. Veröff. Inst. Meeresk. Univ. Berl., N.F., A, *20*: 1–64.

Wüst, G. and A. Defant. 1936. Atlas zur Schichtung und Zirkulation des Atlantischen Ozeans. Schnitte und Karten von Temperatur, Salzgehalt und Dichte. Wiss. Ergebn. dtsch. atlant. Exped. —"Meteor", *6*(Atlas): I–CIII.

Wyrtki, K. 1962. Geopotential topographies and associated circulation in the western South Pacific Ocean. Aust. J. Mar. Freshwat. Res., *13*(2): 89–105.

Wyrtki, K. 1971. Oceanographic atlas of the International Indian Ocean Expedition. The National Science Foundation, Washington, D.C., 531 pp.

Yoshida, K. and T. Kidokoro. 1967. A subtropical countercurrent (II)–A prediction of eastward flows at lower subtropical latitudes. J. Oceanogr. Soc. Japan, *23*(5): 231–246.

Received: *23 October, 1974*; revised: *5 February, 1975.*